Sensors and Materials, Vol. 35, No. 8 (2023) 2855–2870
MYU Tokyo

S & M 3360

Selection of Materials Combined with Optimal Structural Design for Electronically Commutated Permanent Magnet Motor

Guan-Ming Chen,[1] Ching-Chien Huang,[2,3*] and Chien-Ming Huang[1]

[1]Green Energy & System Integration, Research & Development Dep., China Steel Corporation,
No. 1, Zhonggang Rd., Xiaogang Dist., Kaohsiung City 812401, Taiwan (R.O.C.)
[2]Dep. of Mechanical Engineering, National Kaohsiung University of Science and Technology,
No. 415, Jiangong Rd., Sanmin Dist., Kaohsiung City 80778, Taiwan (R.O.C.)
[3]New Materials Research & Development Dep., China Steel Corporation,
No. 1, Zhonggang Rd., Xiaogang Dist., Kaohsiung City 812401, Taiwan (R.O.C.)

(Received February 8, 2023; accepted May 11, 2023; online published May 30, 2023)

Keywords: nonoriented electrical steel, magnet, Hall-effect sensor, EC motor, air conditioning

In this paper, we present the development of a high-efficiency electronic commutated (EC) motor using nonoriented electrical steel produced by China Steel Corporation for window-type air-conditioning system applications. The EC motor combines the highly efficient brushless DC electric motor, Hall-effect sensor, driver, and AC/DC converter, but it has similar volume and equivalent performance to the traditional AC motor. By analyzing the material properties and using simulation tools, an EC motor with a high efficiency of about 82–86.4% is demonstrated in this study. A system manufacturer can replace the AC motor with an EC motor directly in the air-conditioning system for higher performance and save more energy, without altering the mechanical design.

1. Introduction

Energy shortage and environmental protection are the two major issues that humans face today, and motors that bring convenience to humans consume a large amount of energy. Therefore, improving the motor efficiency and reducing power consumption are urgent problems that need to be solved. Recently, permanent magnet brushless DC (PM BLDC) motors are being widely used.[(1–9)] These motors have many advantages, such as having a rotor without additional windings or brushes, simple structure, high operating efficiency, and easy maintenance. Compared with AC motors that provide traditional commercial power, BLDC motors must also have a Hall-effect sensor and a power converter as an intermediate medium. In addition to increasing the complexity and volume of the product, this also increases the complexity of the design. Therefore, the market of motors for home appliances that use commercial power input, including air-conditioning and refrigeration systems that require continuous operation or home/industrial motors that require long-term operation, is still dominated by induction motors. In recent years, in response to the energy-saving requirements of the United States for ENERGY

*Corresponding author: e-mail: huangcc@nkust.edu.tw
https://doi.org/10.18494/SAM4348

ISSN 0914-4935

STAR,[10] the manufacturers of air-conditioning systems have become willing to use BLDC motors to meet the energy efficiency requirements for electric motors of the whole machine. Therefore, electronic commutated (EC) motors that can incorporate BLDC motors and power converters have the opportunity to access this new market. An EC motor is a niche product integrating a high-efficiency and energy-saving BLDC motor, a Hall-effect sensor, the function of speed control, and an AC-to-DC converter, and is of similar size to AC motors with the same specifications, so it can be directly applied to products with AC power input. The main voltage, i.e., AC, is rectified by the electronic commutator of the EC motor. The downstream inverter provides the motor voltage via a DC signal, depending on the specified load. Compared with AC asynchronous motors, EC motors are synchronous, which avoids slip losses and provides a higher efficiency over a wider speed range.[11] The speed of the EC motor depends on the DC voltage supplied to the motor through an inverter module, similar to the principle of managing a frequency converter. However, the motor's electronics are different in that they control which phase of the stator current is applied depending on the position and direction of rotation. EC motors have many advantages[11–15] such as very high efficiency, integrated control (continuous control), very simple plug-and-play connection, and additional functions through the addition of accessories (e.g., control of pressure, flow, speed, temperature, and air quality, tachometer, and alarms). They also have a smaller size, the same performance as AC motors, and lower energy costs, and they are suitable for all countries worldwide. In other words, the original air-conditioning products using AC motors do not require any modification of the control circuit of the system or the internal mechanical design of the product. By installing the EC motor, the efficiency can be improved immediately and the effect of frequency conversion and power saving can be achieved, which is in line with the current trend of energy saving and carbon reduction in various countries. However, to meet the limitation of the same size as AC or BLDC motors under the same specifications, the sizes of the motor and power converter of EC motors must be compressed simultaneously, which is a major challenge to the motor design and the selection of key materials for the motor. More importantly, the problems related to the integrated design technology of the Hall-effect sensor, DC drive loop, and voltage converter must also be overcome, making overall cost control another key factor.[15–32] In this study, the stator core was wire-cut and combined with 3D-printed upper and lower winding frames for a practical preliminary prototype design. A commercial design of an EC motor capable of meeting size constraints, cost constraints, and output performance requirements has been realized.

2. Research Background and Technical Feasibility Analysis

2.1 Research background

In this work, several EC products with excellent sales in the market are analyzed, including Ebm-papst (US), AXAIR (United Kingdom), ZIEHL (Germany), SUNON (Taiwan), Storm (China), and Dunli (China). In addition, the above-mentioned representative Ebm-papst, SUNON, and Storm EC products were actually purchased for sample disassembly and further analysis. Among them, Ebm-papst occupies the leading brand position in the EC motor market.

It is also the industry's first example of integrating the BLDC motor and power converters into the same volume as AC motors with the same output specifications. The main technical threshold of Ebm-papst comes from its excellent motor design, mechanism design, and circuit integration. Its outstanding injection molding technology also provides the excellent vibration and noise quality of this product, so the prices of Ebm-papst EC products are all on the high side. Compared with the expensive Ebm-papst, the motor manufacturers of Taiwan and China have recently successively launched competitive products, namely, SUNON and Storm, respectively, with performance equivalent to that of Ebm-papst at only 20–50% of the cost, which not only enhances the EC motor market sales volume but also increases the willingness of system manufacturers to replace AC motors with EC motors.

In this work, we utilize the data of market analysis and customer feedback to formulate EC motor development specifications and analyze the power wattage of Ebm-papst and Storm products that are similar to those of the motor that will be developed. Through these analyses, we can understand the key materials of the motor and the cost of electronic components, and can also avoid designing a product that infringes on the patents of other manufacturers. According to the analysis results, this type of motor uses 0.35-mm-thick electrical steel and ferrite magnets, and it was found that a height of about 25 mm needs to be reserved for electronic parts under the iron core. Therefore, on the basis of the AC motor of an air conditioner, which will be replaced in this work, the following four points can be summarized from its performance, price, and sample analysis results.

- In addition to the specific benefits of improving the energy efficiency of the air conditioner, the adjustable speed is also another advantage of the EC motor.
- When the fan speed increases, the heat dissipation capacity of the air conditioner is expected to increase proportionally to it, but the increase in power consumption is far less than that of an AC motor.
- In an application environment of relatively high speed, the ability and energy-saving effect of the EC motor are more significant than those of the AC motor.

If the EC motor can effectively improve the overall energy efficiency of the system, and its cost can be reduced to only 3 to 5 times that of the AC motor, the readiness of system manufacturers to replace the EC motor will be improved. Therefore, to achieve this performance and cost objective, aside from upgrading the key materials of the motor, improvements of the motor design and power supply/drive circuit integration technology are the additional focal points of this work.

2.2 Analysis of technical feasibility

In this work, a commercially available BLDC fan motor is introduced into the air-conditioning system and its load is analyzed. Then the specifications of the currently used AC motors are compared to determine the motor specifications to be developed in this research. The currently used AC motor is a Broad-Ocean (China Electric Motor Manufacturers) AC motor (Y5S413B5107), as shown in Fig. 1. The size of its mechanism is Ø96 × 78 mm, and its performance test data are shown in Table 1. As shown in Fig. 2, in this work, we also analyze a

Fig. 1. (Color online) AC motor for window-type air conditioner.

Table 1
Performance test data of Broad-Ocean AC motor (Y5S413B5107).

Motor Speed (rpm) [Measured]	τ (Nm) [Estimated]	P_{out} (W) [Estimated]	P_{in} (W) [Measured]	V [Estimated]	A [Measured]	η (%)
1280	0.235	31.53	80.70	229.915	0.351	39.1
1570	0.348	57.20	96.75	272.535	0.355	59.1

Fig. 2. Commercially available plastic-encapsulated BLDC motor.

commercially available plastic-encapsulated BLDC motor with similar motor power (motor in outdoor units, stator size: Ø88 × 13 mm), which is made of 50CS290 nonoriented electrical steel [produced by China Steel Corporation (CSC)] and JBL 6N grade ferrite magnets. The results of the performance evaluation of this commercially available plastic-encapsulated BLDC motor are shown in Table 2. From Table 2, it can be seen that the efficiency (η) of this BLDC motor is only between 68.5 and 71.9%. To achieve the expected 5–6% increase in overall air-conditioning system efficiency, the performance of the EC motor must reach 79–81%. Therefore, the specifications of the EC motor to be developed in this study are set as shown in Table 3. Since the efficiency of the motor driver is generally about 92–95%, the efficiency of this voltage power converter is about 95–96%, so it is assumed that the efficiency of the BLDC motor to be

Table 2
Results of performance estimation of commercially available plastic-encapsulated BLDC motor.

Motor Speed (rpm) [Measured]	τ (Nm) [Estimated]	P_{out} (W) [Estimated]	P_{in} (W) [Measured]	V [Estimated]	A [Measured]	η (%)
1280	0.235	31.53	46.0	117.949	0.390	68.5
1570	0.348	57.20	79.6	125.75	0.633	71.9

Table 3
Target specifications of EC motor to be developed in this work.

Motor Speed (rpm) [Measured]	τ (Nm) [Estimated]	P_{out} (W) [Estimated]	P_{in} (W) [Measured]	η (%)
1280	0.235	31.53	40.2	78.5
1570	0.348	57.20	69.8	81.9

developed in this work must be at least 89.8% (@ 1280 rpm) to 93.7% (@ 1570 rpm). In view of this, the power density of the EC motor must be higher than that of the BLDC motor shown in Fig. 2 in order to have a sufficient margin of power density to accommodate the integrated circuit board of the motor drive and power conversion circuits. Taking the size of the Broad-Ocean AC motor as the design limit, we first use AutoCAD to draw the 2D layout and then redesign the BLDC motor stator and rotor in accordance with this size. In addition, considering the current height of electronic components and the reserved space for the safety requirements of the power supply board, the preliminarily planned size of the motor and electronic spaces is Ø96 × 39 mm. According to this size specification, the space inside the motor that can accommodate the stator and rotor is designed, and then considering the size of the winding frame and the space reserved for the upper edge of the end cover and housing, the thickness of the stator is initially estimated to be 22 mm. Finally, a 3D model of the EC motor is established using Solid Works. At the same time, the model is used to design the stator positioning seat and the winding frame, and the trial assembly is completed by simulation in advance, as shown in Fig. 3. The space between the motor and the driver is set to 1:1.

3. Development of EC Motors for Air Conditioner

3.1 Selection of motor stator and rotor materials

The motor simulation software JMAG-Express is used in this work to analyze the effects of various materials on motor performance. JMAG-Express has a built-in detailed material database of major steel plants in the world, which meets the needs of this work to analyze the impact of electrical steel on motor performance. In addition, we use this software to quickly establish a mathematical model of the motor to accelerate the motor design process on the basis of the motor structure with a stator outer diameter of 93.66 mm and a stator product thickness of 22 mm. The mathematical model is supplemented by the calculation of the motor formula and then input to JMAG-Express to calculate the size of each part of the motor and simulate the performance of various materials corresponding to the motor. It is roughly estimated that the

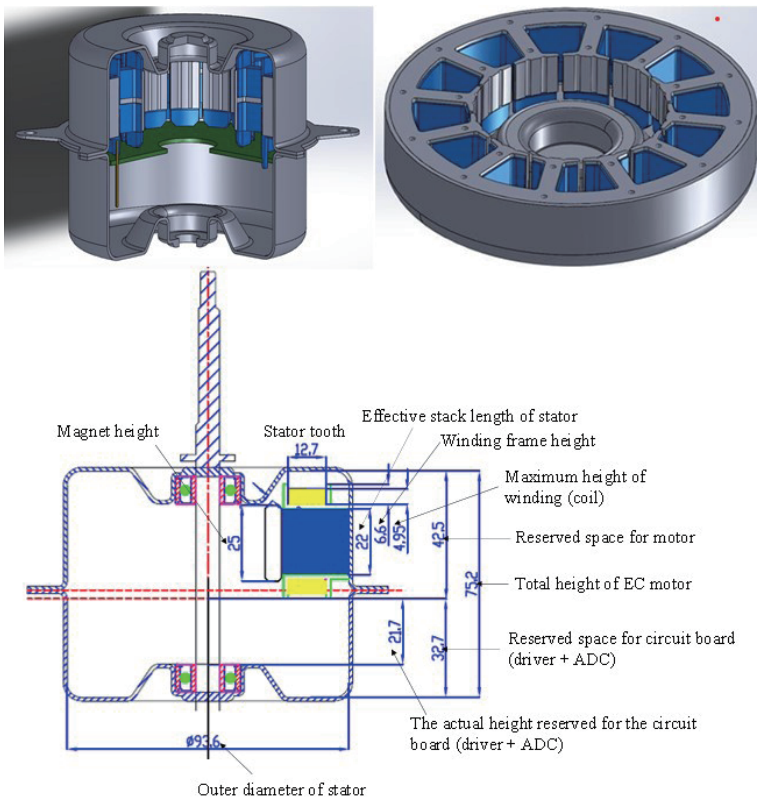

Fig. 3. (Color online) Schematic diagram of internal space design and structure of EC motor.

simulation software cannot simulate the friction loss of mechanical parts (motors at this power level usually have a loss of about 1%). Therefore, the simulated efficiency of the motor must be greater than 91% (@ 1280 rpm) and 94% (@ 1570 rpm) to satisfy the target efficiency set by the EC motor, namely, 89.8% (@ 1280 rpm) and 93.7% (@ 1570 rpm).

Regarding the selection of substrate materials for nonoriented electrical steel, the 0.35 mm electrical steel used in ebm-papst motors was the first to be considered. However, through the simulation analysis of the four substrates 35CS250, 50CS290, 50CS400, and 50CS470, it can be found that these four substrates have little effect on the motor torque, as demonstrated in Fig. 4. In addition, except for 50CS470, the motor efficiencies all exceed 94%, as shown in Fig. 5. Further analysis of the corresponding iron losses of these four electrical steels showed that the highest iron loss of 50CS400 at 1500 rpm is less than 0.8 W, as shown in Fig. 6. To maintain the same motor performance and effectively reduce costs, we use a substrate that is cheaper but with acceptable iron loss, 50CS400, as the material of the EC motor stator in this study. For the calculation of efficiency and iron loss, note that the simulation conditions (speed and corresponding output torque) are set under the working conditions of two rated speeds, as well as the process limit of the slot fullness rate of 65%, and the volume limit. On the basis of the above conditions, the width of the stator teeth is changed to meet the width of the yoke to less than 5 mm of the stamping limit and the conditions of saturation flux of <1.5 Tesla under the working conditions.

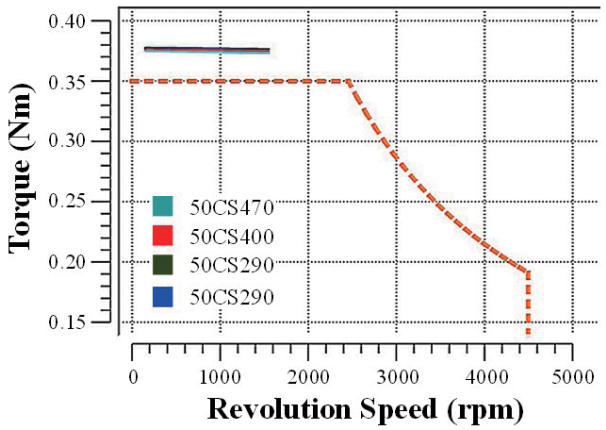

Fig. 4. (Color online) Output torques of the motors made with to the four types of electrical steel.

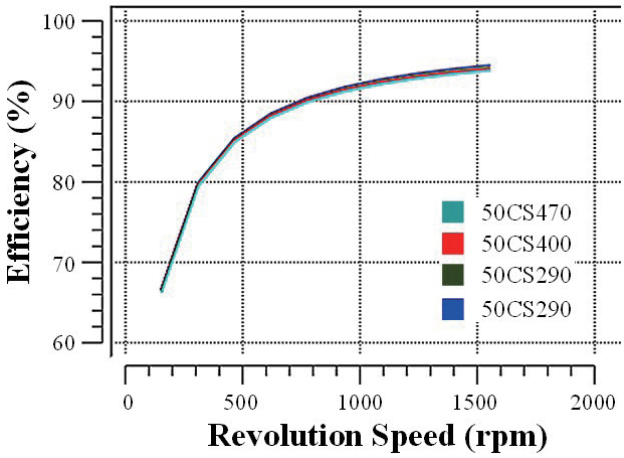

Fig. 5. (Color online) Efficiencies of motors made with the four types of electrical steel.

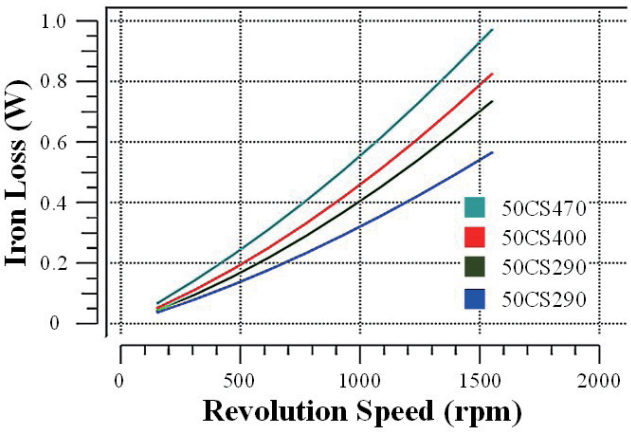

Fig. 6. (Color online) Iron losses of the motors made with the four types of electrical steel.

In terms of magnet selection for the rotor, in this work, we compare the effects of three commercially available 6N-grade ferrite magnets on motor performance considering the overall cost of the motor, stator flux density, and operating temperature requirements. After comparing the simulation results, the output torques of the motors using the three different ferrite magnets were found to be similar, and the motor using the 6N-A magnet has the highest efficiency, as shown in Table 4. It is important to note that because the 6N-grade magnet does not contain the expensive metals La and Co, its material cost is relatively low.

3.2 Design of motor structure

After selecting the key materials on the basis of the above simulation results, JMAG-Express is then used to optimize the motor structure. In the design process, the process limits of general motor manufacturers are also considered, including the stamping accuracy of the stator, the limit of the needle of the winding machine, and the size of the air gap. Figure 7 shows the simulation results of the design of the motor tooth width. To meet the requirements of higher power density, it is necessary to further increase the winding space and slot fill factor of the motor. According to the simulation results, although the motor efficiency does not change clearly when the tooth width is between 3.5 and 4.7 mm, a reduction in tooth width causes the iron loss to increase, and while an increase in tooth width can better suppress the vibration noise. When the tooth width is 4.7 mm, the preset winding space of the motor is exceeded, so the maximum tooth width is set to 4.5 mm. Through simulation, it is found that when the yoke width is reduced from 5 to 3.5 mm, iron loss increases. On the other hand, when the yoke width is increased, the winding space is limited. Therefore, the yoke width is set to 5 mm.

Figure 8 shows the simulation results of the design of the motor yoke width. Since the the magnetic lines of force that pass by the stator yoke are more than half of the stator teeth., the width of the yoke is generally about 50–70% of that of the teeth. However, it is necessary to consider the limitation of the stamping process when designing the stator yoke, and the most suitable size for stamping is 5 mm or more.

After optimizing the motor structure, the JMAG-designer finite element analysis software is used to analyze the magnetic flux of each part of the motor stator to confirm that the working environment of the electrical steel is close to the magnetic flux saturation point and to further determine the optimal size and material of the stator. It is confirmed by simulation calculation that the highest point of stator flux occurs at the knee point of the stator teeth (= 1.4 T), and has

Table 4
Efficiencies of the motors made with to the three types of 6N-grade ferrite magnet.

	6N-T	6N-A	6N-B
Recoil permeability	1.07	1.07	1.07
B_r, Remanence (Gauss)	4400	4382	4278
${}_iH_c$, Coercivity (Oe)	3300	3545	3458
Density (g/cm^3)	5.1	5.1	5.1
Efficiency (%) @1280rpm	**92.86**	**93.09**	**92.88**

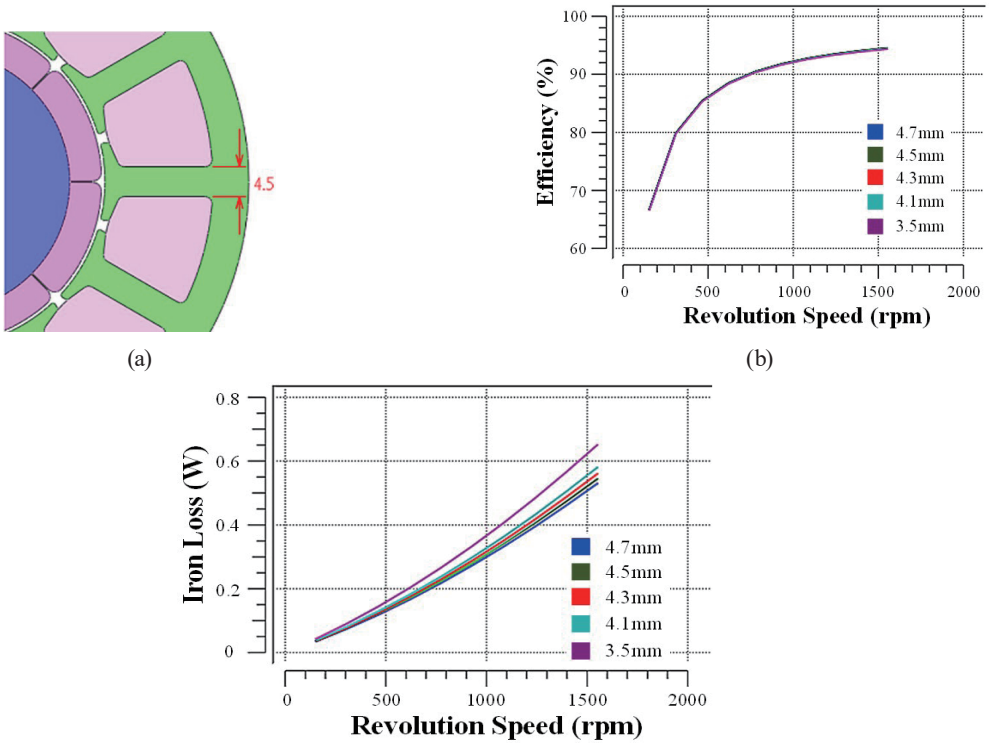

(a) (b)

(c)

Fig. 7. (Color online) Optimized design of motor tooth width: (a) schematic diagram of stator tooth, (b) efficiency output, and (c) iron loss.

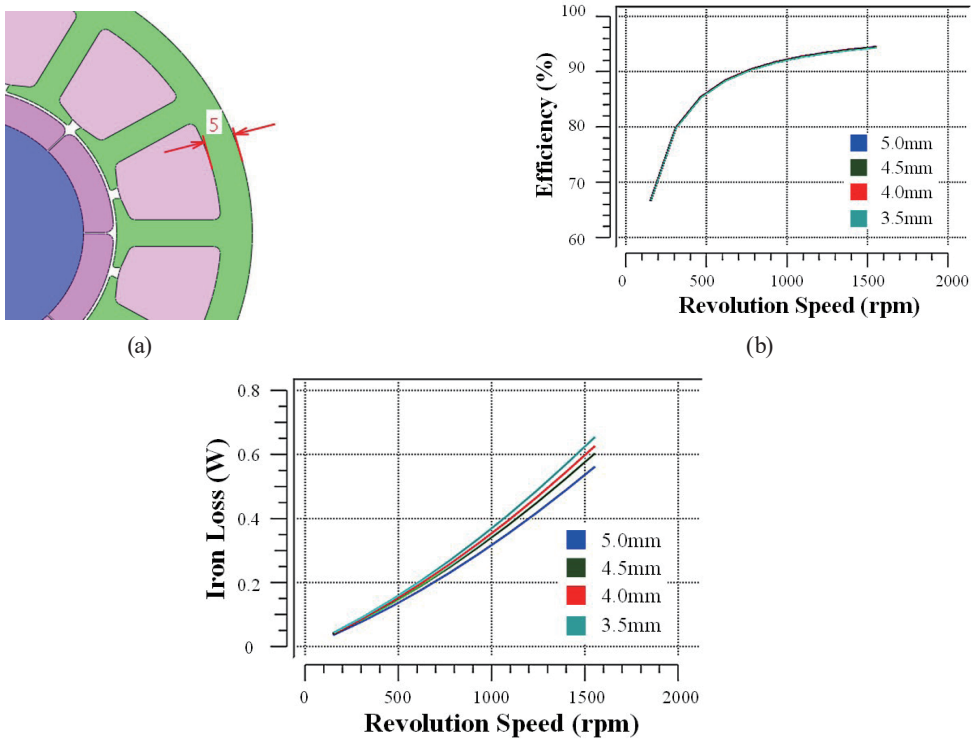

(a) (b)

(c)

Fig. 8. (Color online) Optimized design of motor yoke width: (a) schematic diagram of stator yoke, (b) efficiency output, and (c) iron loss.

not yet caused the magnetic saturation of the iron core. This result indicates that the material of the stator can withstand the electrical loading of this motor, as shown in Fig. 9.

Since the maximum speed of the EC motor is only 1500 rpm and the starting current is not large, the Y-connection of a concentrated winding is adopted. Then, using formulas and simulations, it is calculated that when the slot fullness rate is 65%, the EC motor winding required to achieve the target speed is equal to 0.35 × 337 turns (wire diameter of the 0.35 mm coil). The winding diagram is shown in Fig. 10.

3.3 Integration of Hall-effect sensors and other modules

The EC motor integrates the controller, motor drive, and power conversion circuits into one. Among the key electronic components of EC motors demonstrated in this study, the most critical is the Microcontroller Unit-IC using RICHTEK RT7100 packaged with Thin Shrink Small Outline Package with 28 pins for Hall-effect sensors to detect the position of the rotating magnet. In addition, the Optoisolator Transistor Output-IC uses EL3H7 packaged by Toshiba, the Intelligent Power Module-IC uses INFINEON IRSM505, and the Operational Amplifier-IC uses Texas Instruments LM393AD. The overall layout and printed circuit board assembly (PCBA) are shown in Fig. 11.

3.4 Verification and demonstration of motor

After repeatedly confirming that the motor design is correct using mathematical models and simulation software, the computer-aided design drawing program software AutoCAD is used to make a drawing of the stator. The stator core is obtained by wire cutting and used in combination with 3D-printed upper and lower winding frames for preliminary verification, as shown in Fig. 12. Then, we confirm whether the iron core and the circuit board combination mechanism are

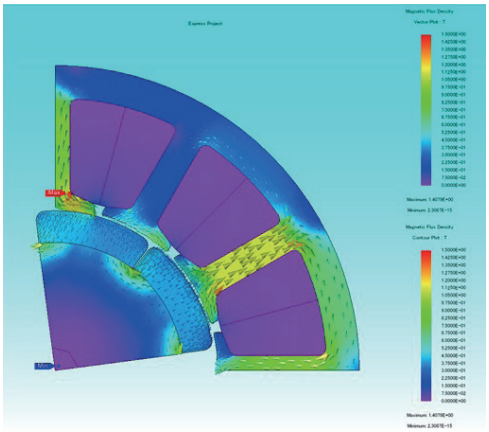

Fig. 9. (Color online) Analysis of magnetic flux in various parts of the motor stator.

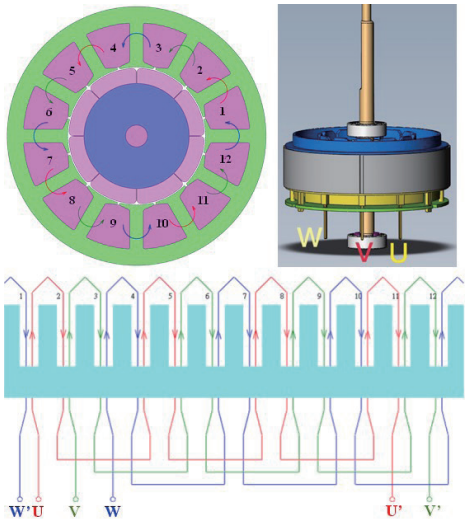

Fig. 10. (Color online) Layout and specifications of EC motor winding.

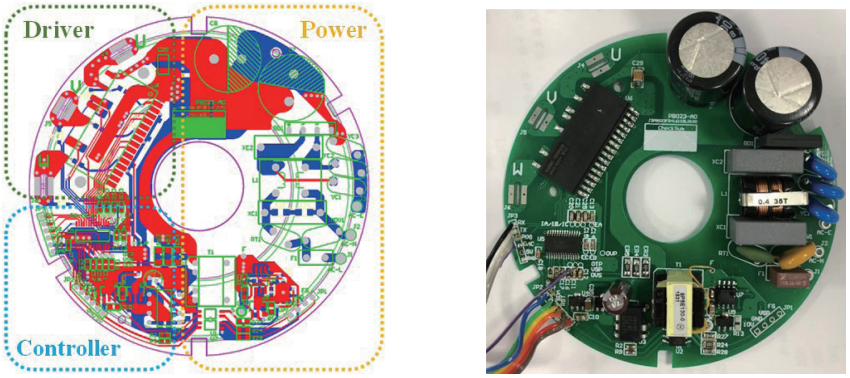

(a) (b)

Fig. 11. (Color online) Controller, motor drive, and power conversion circuits integrated in the EC motor: (a) overall layout and (b) PCBA.

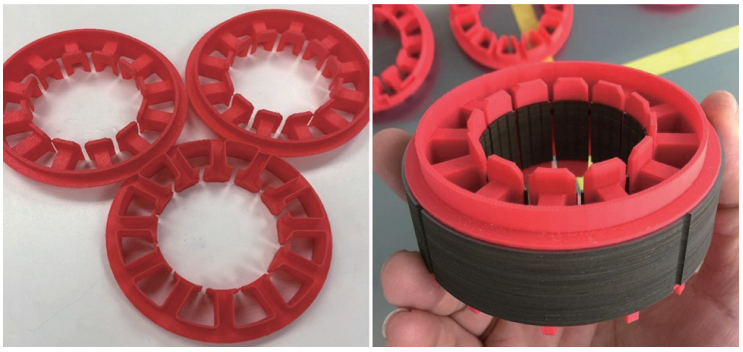

Fig. 12. (Color online) Wire-cut iron core used in combination with 3D-printed upper and lower winding frames for preliminary verification.

correctly designed, as shown in Fig. 13. Finally, the mock-up products of the upper and lower winding frames are machined by computer numerical control (CNC), and the winding is performed in accordance with the designed winding specifications.

Figure 14(a) shows the various mechanical parts and completed winding of the motor stator. It can be seen that there is still room for improvement of the slot fullness rate. However, considering the mass production of the motor in the future and verification of the previous simulation results, we will not further optimize the winding specifications for the time being. Figure 14(b) shows the diagram of the completed EC motor assembly in this work.

3.5 Measurement of EC motor performance

In this work, a trial run test of the EC motor is demonstrated with a pseudofan to test the motor and simulate the load of the fan blade, in order to further debug the layout and adjust the motor drive setting, as shown in Fig. 15. Finally, we use a dynamometer to measure the performance of the motor, as shown in Fig. 16.

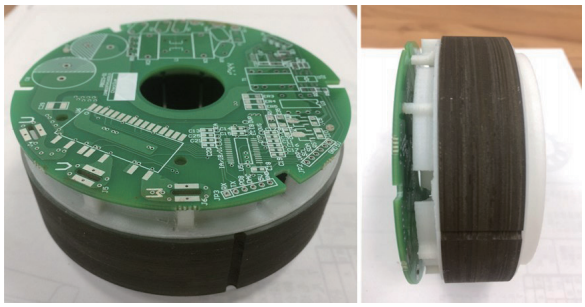

Fig. 13. (Color online) Combination of the upper and lower winding frames and circuit board.

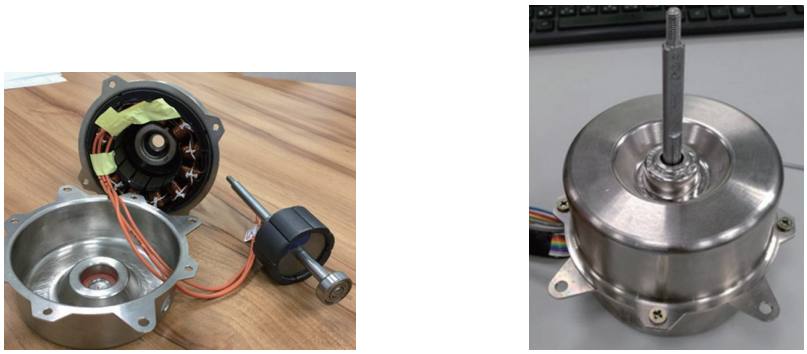

(a) (b)

Fig. 14. (Color online) (a) Various mechanical parts and completed winding of the motor stator, and (b) diagram of the completed EC motor assembly in this work.

Fig. 15. (Color online) The EC motor is equipped with a pseudofan to adjust and optimize the driving parameters.

In this work, the important parameter that determines motor performance is efficiency. As shown in Fig. 17 (*I*: current, *N*: output torque), the speed of the EC motor is 1263 rpm at a torque of 0.232 Nm, which is close to 0.235 Nm at the operating point, and the overall motor efficiency is 82.9%. Under the operating point with a torque of 0.347 Nm, the speed is 1617 rpm and the motor efficiency is 86.4%, which are both better than the preset target values (78.5 and 81.9%). As shown in Fig. 17, when the EC motor is operated with a torque of 0.232 Nm (close to 0.235 Nm at the operating point), the speed is 1263 rpm and the overall motor efficiency is 82.9%. On the other hand, when the EC motor is operated with a torque of 0.347 Nm at the operating point,

Fig. 16. (Color online) Dynamometer for measuring the performance of the motor.

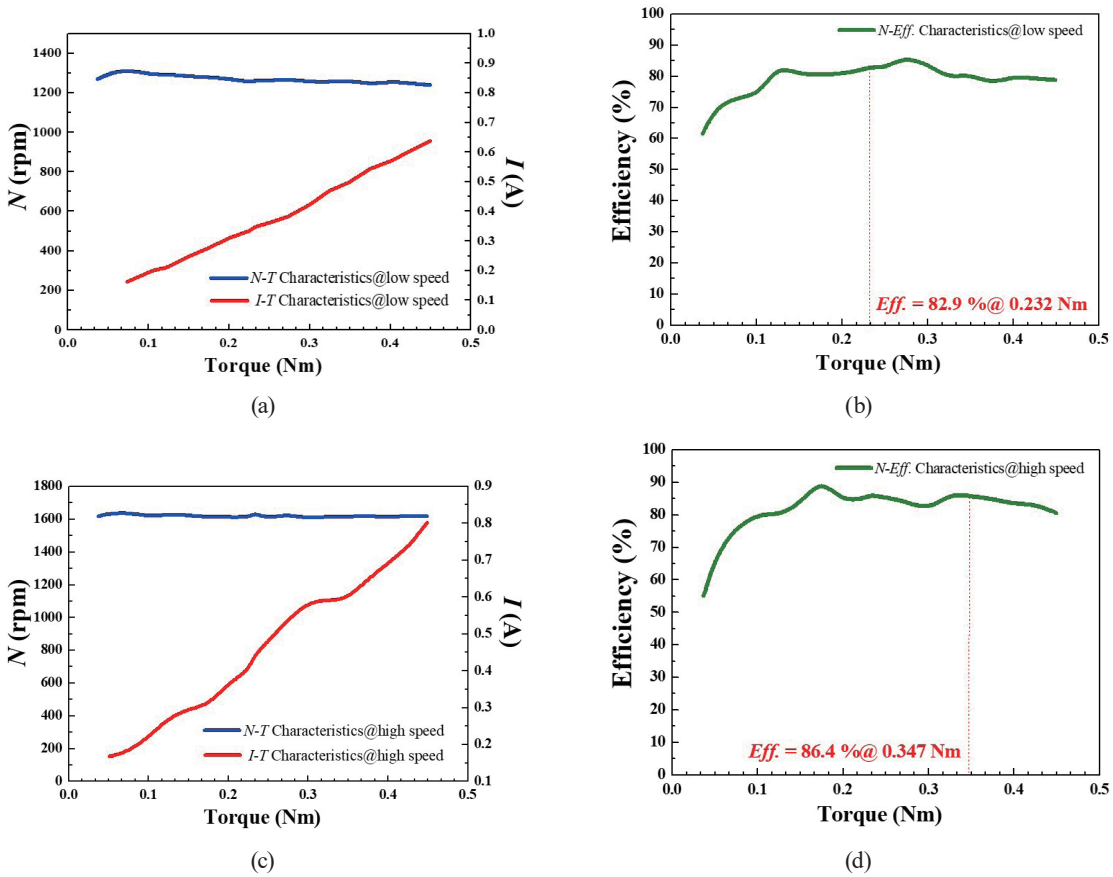

Fig. 17. (Color online) Measured results of EC motor performance: (a) *N*–*T* and *I*–*T* curves at low speed (1280 rpm), (b) efficiency at low speed (1280 rpm), (c) *N*–*T* and *I*–*T* curves at high speed (1570 rpm), and (d) efficiency at high speed (1570 rpm).

the speed is 1617 rpm and the motor efficiency is 86.4%. It can be observed from the above results that the efficiencies of the EC motor demonstrated in this work are better than the target values (78.5 and 81.9%) regardless of whether the EC motor is operated at a low or high speed.

Finally, a rough evaluation of the production cost of the motor was also conducted in this study. By optimizing the motor design to minimize the use of silicon steel sheets and permanent magnets, and further integrating the drive and power circuits to reduce the cost of printed circuit board (PCB) and PCBA, the cost of the EC motor developed in this research becomes about 2.1 times that of the AC motor of the same level, which is far lower than the preset target (3–4 times), indicating that the EC motor developed in this study also has good cost competitiveness.

5. Conclusions

In this work, the material properties, performance, and engineering applications of EC motors are systematically discussed. A high-efficiency EC motor in which nonoriented electrical steel produced by CSC is used as a stator core material was developed using Hall-effect sensors. The effects of electrical steel properties on motor iron loss, copper loss, efficiency, and torque were analyzed using JMAG-Express and JMAG-Designer motor simulation software. Then, a practical preliminary prototype design was implemented by the wire cutting of the stator core and combined with the 3D printing of the upper and lower winding frames. Finally, a prototype EC motor suitable for mass production was developed. As can be seen from the test results, the efficiency of the EC motor demonstrated in this work is higher than the target values (78.5 and 81.9%), regardless of whether it is running at a low or high speed. The overall efficiency of the motor was 82.9% when the EC motor had a torque of 0.232 Nm near the operating point (0.235 Nm at the operating point) and reached a speed of 1263 rpm. Furthermore, when the EC motor was operated with a torque of 0.347 Nm at the operating point and reached a speed of 1617 rpm, the motor efficiency obtained 86.4%. In addition, a rough evaluation of the production cost of this motor was conducted in this study. The cost of the EC motor developed in this study is about 2.1 times that of an AC motor of the same class, which is much lower than the preset target (3 to 4 times), indicating that the EC motor developed in this study is also competitive in terms of cost. As a result, a commercial design that can meet the size constraints, cost constraints, and output performance requirements is realized. In the future, the relevant findings of this study will also be applicable to other household appliances that require long-term operation, such as vertical fans, air purifiers, water-cooled fans, and water pumps, as well as to industrial motor products. It is believed that they can all achieve satisfactory synergistic results in terms of energy and carbon reduction.

Acknowledgments

This work is partially supported by the National Science and Technology Council, Taiwan, under NSTC 110-2222-E-992-001.

References

1 J. R. Hendershot and T. J. E. Miller: Design of Brushless Permanent-Magnet Motors (Oxford University Press, UK, 1995) Chap. 1.
2 D. C. Hanselman: Brushless Permanent Magnet Motor Design (Writers' Collective, U.S., 2003) 2nd ed., Chap. 2.

3 I. Petrov and J. Pyrhonen: IEEE Trans. Ind. Electron. **60** (2013) 2131. https://doi.org/10.1109/TIE.2012.2191757
4 P. Akiki, M. Hage-Hassan, P. Dessante, J.-C. Vannier, and M. Bensetti: 2017 IEEE Int. Electric Machines and Drives Conf. (IEMDC, 2017) 1. https://doi.org/10.1109/IEMDC.2017.8002060
5 P. Lindh, I. Petrov, J. Pyrhönen, and T. Santa-Nokki: 2019 IEEE Int. Electric Machines and Drives Conf. (IEMDC, 2019) 721. https://doi.org/10.1109/IEMDC.2019.8785353
6 A. J. Kanapara and K. P. Badgujar: 2020 IEEE 21th National Power Systems Conf. (NPSC, 2020) 1. https://doi.org/10.1109/NPSC49263.2020.9331855
7 O. Dobzhanskyi, O. Duniev, E. Amiri, A. Yehorov, P. Gottipati, A. Masliennikov, and E. Mendrela: 2021 IEEE 2nd KhPI Week on Advanced Technology (KhPIWeek, 2021) 346. https://doi.org/10.1109/KhPIWeek53812.2021.9569983
8 Q. Zhi, L. Shen, C. Zhu, and S. Yan: 2022 IEEE 4th Int. Conf. Intelligent Control, Measurement and Signal Processing (ICMSP, 2022) 587. https://doi.org/10.1109/ICMSP55950.2022.9859009
9 B. Zheng, Z. Zhang, T. Shi, Y. Cao, and C. Xia: 2022 IEEE 23rd Int. Conf. Computation of Electromagnetic Fields (COMPUMAG, 2022) 1. https://doi.org/10.1109/COMPUMAG55718.2022.9827506
10 ENERGY STAR: https://www.energystar.gov/ (accessed February 2023).
11 AIR CURTAINS SPECIALIST - INDUSTRIAL VENTILATION: https://www.airtecnics.com/news/how-ec-motors-work-and-what-are-their-advantages (accessed March 2023).
12 Y. Chen, B. Luo, Q. Zhang, and Y. Fang: 2021 3rd Int. Academic Exchange Conf. Science and Technology Innovation (IAECST, 2021) 930. https://doi.org/10.1109/IAECST54258.2021.9695651
13 L. Lavrinovicha, J. Dirba, K. Sejejs, and E. Kamolins: Latv. J. Phys. Tech. Sci. **56** (2019) 3. https://doi.org/10.2478/lpts-2019-0008
14 P. Yin and M. B. Pate: J. Build. Eng. **22** (2019) 305. https://doi.org/10.1016/j.jobe.2018.12.016
15 B. D. Cullity and C. D. Graham: Introduction to Magnetic Materials (Wiley-IEEE Press, U.S, 2008) 2nd ed., Chap 3. https://doi.org/10.1002/9780470386323
16 J. F. Gieras and M. Wing: Permanent Magnet Motor Technology-Design and Applications (CRC Press, U. S., 2008) 2nd ed., Chap. 2.
17 M. Amar and R. Kaczmarek: IEEE Trans. Magn. **31** (1995) 2504. https://doi.org/10.1109/20.406552
18 Y. C. Chuang: Development of Eddy-current Displacement Sensor and Research on Multi-degrees Displacement Sensing System (Master Thesis, Department of Mechanical Engineering, National Taiwan University, Taiwan, 2001) Chap. 3. https://hdl.handle.net/11296/6643r4
19 S. Yanase, H. Kimata, Y. Okazaki, and S. Hashi: IEEE Trans. Magn. **41** (2005) 4365. https://doi.org/10.1109/TMAG.2005.854863
20 K. Koibuchi, K. Sawa, T. Honma, T. Hayashi, K. Ueda, and H. Sasaki: IEEE Trans. Magn. **43** (2007) 1749. https://doi.org/10.1109/TMAG.2007.892509
21 J. C. Gamazo-Real, E. Vázquez-Sánchez, and J. Gómez-Gil: Sensors **10** (2010) 6901. https://doi.org/10.3390/s100706901
22 D. Krishnan T. V. Samskriti, and K. P. Vittal: 2015 IEEE 10th Int. Conf. Industrial and Information Systems (ICIIS, 2015) 193. https://doi.org/10.1109/ICIINFS.2015.7399009
23 A. Usman and B. S. Rajpurohit: IEEE Access **7** (2019) 147542. https://doi.org/10.1109/ACCESS.2019.2946694
24 D. L. Oneal and P. Yin: Sci. Technol. Built Environ. **26** (2020) 1165. https://doi.org/10.1080/23744731.2020.1787084
25 Z. Wang, Z. Han, L. Ding, and G. Wang: Sci. Technol. Built Environ. **27** (2020) 329. https://doi.org/10.1080/23744731.2020.1797443
26 F. Naseri, E. Farjah, E. Schaltz, K. Lu, and N. Tashakor: IEEE Trans. Circuits Syst. I: Regul. Pap. **68** (2021) 1308. https://doi.org/10.1109/TCSI.2020.3043468
27 X. Anitha Mary, E. Jesintha, P. Rajalakshmy, and G. Manoj: AIP Conf. Proc. (AIP, 2022) 020007. https://doi.org/10.1063/5.0130995
28 S. Manglik and A. Garg: Proc. 6th Int. Conf. Exhibition on Smart Grids and Smart Cities (Springer, Singapore, 2022) 327–339. https://doi.org/10.1007/978-981-16-9008-2
29 Y. Özüpak: J. Brilliant Eng. **3** (2022) 4658. https://www.acapublishing.com/dosyalar/baski/BEN_2022_658.pdf
30 J. Cai, X. Zhang, W. Zhang, and Y. Zeng: IEEE Trans. Ind. Electron. **37** (2022) 8322. https://doi.org/10.1109/TPEL.2022.3144897
31 D. Kumar, S. D. Choudhary, M. Tabrez, A. Ayob, and M. S. H. Lipu: Energies **15** (2022) 7823. https://doi.org/10.3390/en15217823
32 D. Mohanraj, R. Aruldavid, R. Verma, K. Sathiyasekar, A. B. Barnawi, B. Chokkalingam, and L. Mihet-Popa: IEEE Access **10** (2002) 54833. https://doi.org/10.1109/ACCESS.2022.3175011

About the Authors

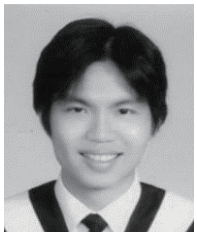

Guan-Ming Chen received his Ph.D. degree in electrical engineering from National Sun Yat-sen University, Kaohsiung, Taiwan, in 2012. From 2013 to 2015, he served as an engineer at Sunonwealth Electric Machine Industry Co., Kaohsiung, Taiwan. In 2015, he joined the Department of Green Energy & System Integration, China Steel Corporation, Kaohsiung, Taiwan, as a research scientist. His areas of interest include electric machine design, drives, and mechatronics. (189837@mail.csc.com.tw)

Ching-Chien Huang received his Ph.D. degree in electronics engineering from National Chiao-Tung University, Hsinchu, Taiwan, in 2009. From 2010 to 2012, he served as a principal engineer at Taiwan Semiconductor Manufacturing Co. In 2012, he joined the Department of Research & Development, China Steel Corporation, Kaohsiung, Taiwan, as a research scientist. He is currently an assistant professor at the Department of Mechanical Engineering, National Kaohsiung University of Science and Technology, Kaohsiung, Taiwan. He has published over 30 journal papers and 10 patents. His research is focused on electric machine design and magnetic materials. (huangcc@nkust.edu.tw)

Chien-Ming Huang was born in Kaohsiung, Taiwan, in 1978. He received his M.S. and Ph.D. degrees in electrical engineering from National Cheng Kung University, Tainan, Taiwan, in 2003 and 2008, respectively. From 2011 to 2015, he was an assistant manager of the Research and Design Department at Ablerex Electronics, Taiwan. Since 2015, he has been an R&D engineer in the Department of Green Energy & System Integration, China Steel Corporation, Kaohsiung, Taiwan. His research interests are in power electronics and energy conversion. (185082@mail.csc.com.tw)